LA-UR- 97-3100

Approved for public release; distribution is unlimited.

Title: APPLICATION OF 2-D SIMULATION TO HOLLOW Z-PINCH IMPLOSIONS

Author(s): Darrell L. Peterson, XPA
Richard L. Bowers, XPA
John H. Brownell, XTA
Carl Lund, XPA
Walter Matuska, XPA
Kelly McLenithan, XPA
Henn Oona, DX-3
C. Deeney, M. Derson, R. Spielman, T Nash, G. Chandler, R. Mock, T.W. L. Sanford and M. K. Matzen (Sandia)
Norman F. Roderick. UNM

Submitted to: FOURTH INTERNATIONAL CONFERENCE ON DENSE Z-PINCHES
MAY 28-30, 1997
VANCOUVER, CANADA

MASTER

Los Alamos
NATIONAL LABORATORY

DISCLAIMER

LA-UR- 97-3100
CONF-9705120--

Application of 2-D Simulations to Hollow Z-Pinch Implosions[1]

D. L. Peterson, R. L. Bowers, J. H. Brownell, C. Lund, W. Matuska, K. McLenithan and H. Oona
Los Alamos National Laboratory, Los Alamos, NM, 87545

C. Deeney, M. Derzon, R. B. Spielman, T. J. Nash, G. Chandler, R. C. Mock, T. W. L. Sanford and M. K. Matzen
Sandia National Laboratory, Albuquerque, NM, 87185

N. F. Roderick
University of New Mexico, Albuquerque, NM, 87131

Abstract. The application of simulations of z-pinch implosions should have at least two goals: first, to properly model the most important physical processes occurring in the pinch allowing for a better understanding of the experiments and second, provide a design capability for future experiments. Beginning with experiments fielded at Los Alamos on the Pegasus I and Pegasus II capacitor banks, we have developed a methodology for simulating hollow z-pinches in two dimensions which has reproduced important features of the measured experimental current drive, spectrum, radiation pulse shape, peak power and total radiated energy (1,2,3). This methodology employs essentially one free parameter, the initial level of the random density perturbations imposed at the beginning of the 2-D simulation, but in general no adjustments to other parameters (such as the resistivity) are required (1). Limitations in the use of this approach include the use of the 3-T, gray diffusion treatment of radiation and the fact that the initial perturbation conditions are not known *a priori*. Nonetheless, the approach has been successful in reproducing important experimental features of such implosions over a wide variety of timescales (tens of nanoseconds to microseconds), current drives (3 to 16 MA), masses (submilligram to tens of milligrams), initial radii (<1 cm to 5 cm), materials (Al and W) and initial configurations (thin foils and wire arrays with 40 to 240 wires). Currently we are applying this capability to the analysis of recent Saturn and PBFA-Z experiments (4,5). The code results provide insight into the nature of the pinch plasma prior to arrival on-axis, during thermalization and development after peak pinch time. Among other things, the simulation results provide an explanation for the production of larger amounts of radiated energy than would be expected from a simple slug-model kinetic energy analysis and the appearance of multiple peaks in the radiation power. The 2-D modeling has also been applied to the analysis of Saturn "dynamic hohlraum" experiments and is being used in the design of this and other Z-Pinch applications on PBFA-Z.

---

[1] Work Supported by DOE.

INTRODUCTION

Two-dimensional Radiation-Magnetohydrodynamic (RMHD) simulations of hollow z-pinches should provide both physical insight into the important processes leading to radiation production as well as allow for the reliable design of new experiments. To fulfill this role, the RMHD codes must accurately reproduce the important experimental features seen in z-pinch implosions. In this paper we will describe simulations with a 2-D Eulerian RMHD code (1) which has been benchmarked with other codes and experiments on the Los Alamos Pegasus I and Pegasus II capacitor banks, the Procyon explosive generator system (1,2,3) and the Sandia Saturn and PBFA-Z accelerators (4,5).

Imploding z-pinch plasmas are susceptible to the magnetically driven analog of classical Rayleigh-Taylor fluid instabilities. Significant differences from the hydro-only instabilities arise in that instability growth in the azimuthal direction is much reduced from that in the axial direction, allowing for greater applicability of 2-D codes using cylindrical symmetry, and that there is only one fluid (the plasma), with the driving magnetic field (which plays the part of the "light" fluid) penetrating the plasma. Thus there are no interfaces as such and the instability is not easily characterized in spike-to-bubble amplitude. The magnetic field is also not tied to particular fluid elements but to resistivity and the current may flow at various times through different regions of the plasma spikes and bubbles.

The presence of instabilities degrades the performance of the radiation production from that which could be expected from 1-D simulations. Initially, the plasma will be spread over a larger radial extent by the growth of spike and

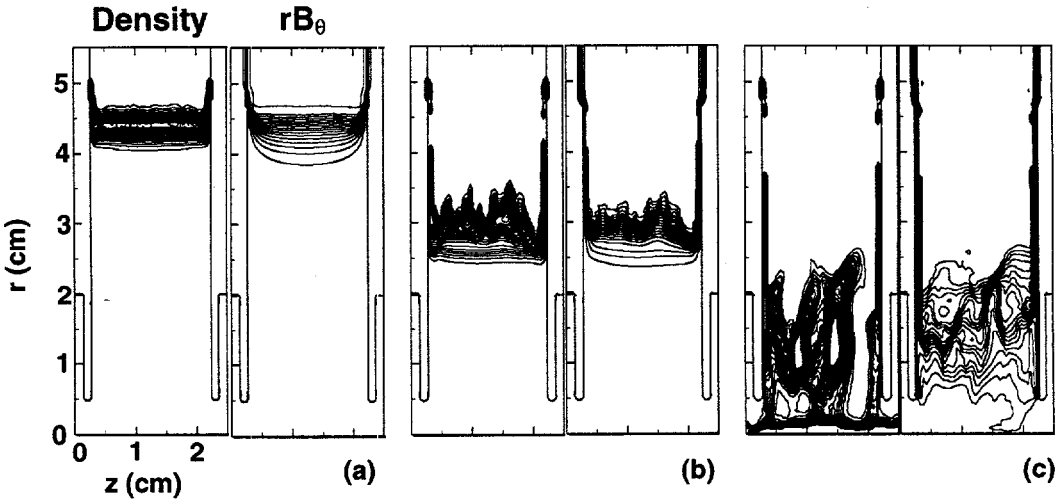

Figure 1. Contours of density and rB_θ for three times in a simulation of the Pegasus II-25 experiment. By the last time shown (c), the bubble region located near the right electrode has burst through the plasma shell. This occurrence is evidenced in the measured load current and is coincident with the onset of the radiation pulse.

bubble regions as well as suffering a loss of axial uniformity. This thickening of the imploding shell is followed by the bubble regions thinning to such an extent that the bubbles may burst through the shell accelerating material and magnetic field to the axis if the disruption is severe enough. This is illustrated in Fig. 1, which shows instability development in density and magnetic field for a simulation of the Pegasus II-25 experiment. This experiment used a 2-cm long, 10-cm diameter, 14.3 mg cylindrical Al foil. The peak drive current of 5.1 MA resulted in a 2 μs implosion time and a radiation pulse with a FWHM of about 200 ns. The simulation reproduced features seen in optical framing camera photographs and the experimentally measured current as well as generating a radiation pulse of the correct total energy and very similar pulse duration and shape as that measured in the experiment (3). The methodology used in such simulations is to begin the 2-D simulations using the current and velocity determined from a 0-D (slug) calculation at a point when the plasma has imploded 2% of the distance to the axis from the initial radius. The 2-D plasma begins as a slab with random perturbations imposed upon a uniform density profile. The perturbation level for the simulation in Fig. 1 is 15% (i.e. the densities in the plasma zones vary between $0.85\times\rho_0$ and $1.15\times\rho_0$).

INSTABILITY CHARACTERIZATION

Lacking an interface, it is difficult to define a characteristic amplitude for the instabilities, and in addition, the linear theory employed to examine the instability development is inapplicable after a very short time. A typical implosion time will be many (tens to hundreds) of instability e-folding times which eliminates this description as useful in characterizing the instability growth. With only a single material involved in instability development, measures such as mixing layer thickness are also difficult to apply and of limited utility. In the simulations discussed here, the most important event in the instability development is the breakthrough of the plasma shell. Consequently, we introduce a measure of the instability growth termed "fractional involved mass," ΔM, which allows a characterization of the instability growth, defined as follows:

$$\Delta m = 2\pi \iint \left| \rho(r,z) - \bar{\rho}(r) \right| r dr dz , \tag{1}$$

$$\bar{\rho}(r) = \frac{\int \rho(r,z) dz}{\int dz} , \tag{2}$$

$$\Delta M = \frac{\Delta m}{M} , \tag{3}$$

where M is the total mass of imploding shell. In addition, it is useful to define a "fractional distance traveled," ΔX:

$$\Delta X = \frac{r_0 - \bar{r}(t)}{r_0}, \tag{4}$$

with $\bar{r}(t)$ being the mass-averaged shell radius. The quantity ΔM can be visualized as a measure of the fraction of the imploding shell which is either contributing to the above-average density in spike regions or missing from the below-average density of bubble regions. In practice, the maximum values of ΔM range between about 0.8 and 1.2, and a peak in this quantity represents a maximum in the instability development at that time. In Fig. 2, the fractional involved mass measure is shown as a function of fractional distance traveled for the calculation pictured in Fig. 1. The breakthrough of the plasma shell by the most developed bubble feature (near the right electrode) is seen as the peak in the fractional involved mass and occurs slightly prior to the time shown in Fig. 1c.

SATURN SIMULATIONS

Using the methodology developed in simulating the Los Alamos Pegasus I, Pegasus II and Procyon experiments, simulations were made of tungsten and aluminum implosions on the Sandia Saturn accelerator. In an experiment using 90

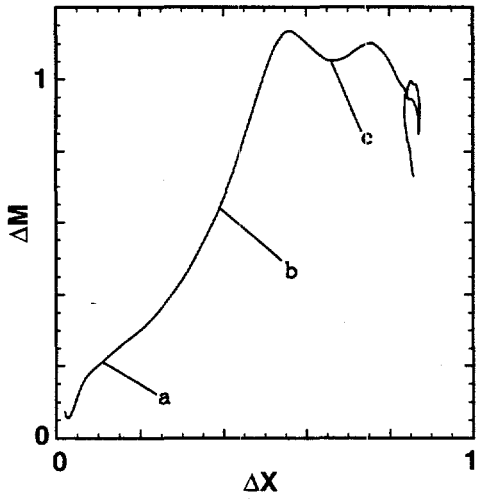

Figure 2. Fractional involved mass vs fractional distance traveled for the Pegasus II-25 experiment simulation. The points marked a, b and c correspond to the times shown in Fig. 1a, 1b and 1c.

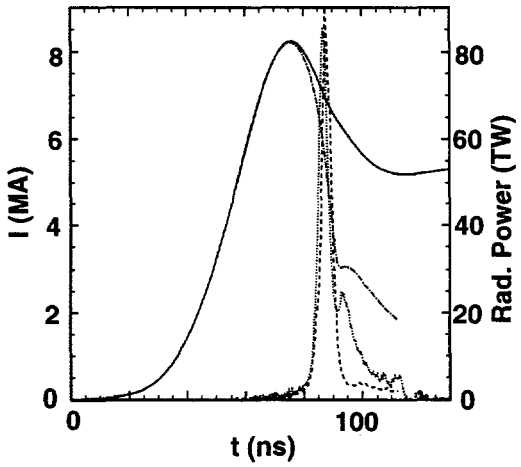

Figure 3. Comparison of experimental (solid, dotted) and simulation (dot-dash, dashed) currents and radiation powers for a 120 wire tungsten Saturn implosion (#2224). Experimental current after the peak is unreliable.

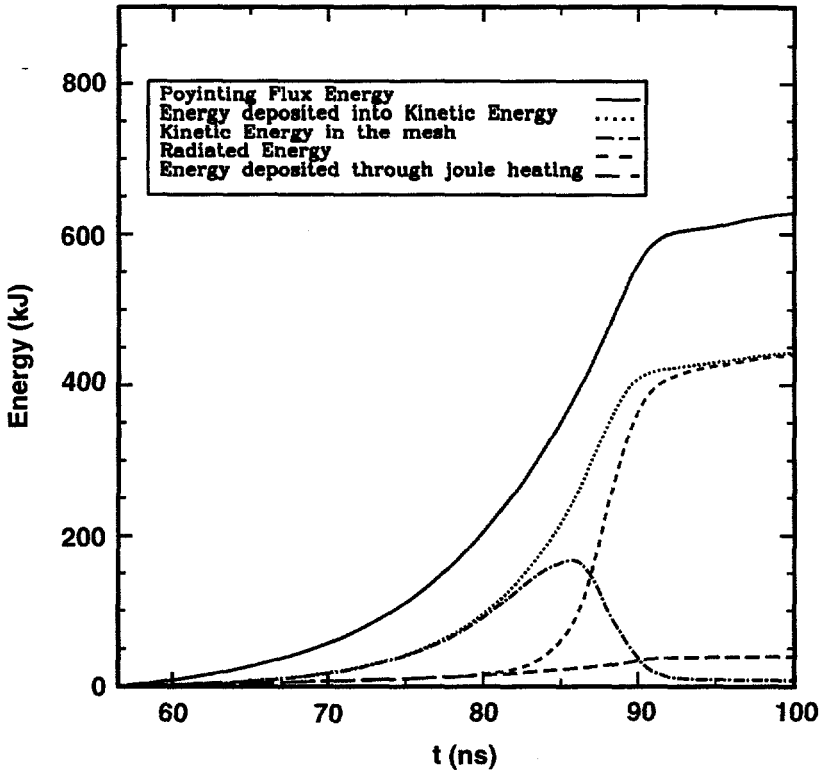

Figure 4. Energy balance and flow in the 2-D simulation of the Saturn 2224 experiment. Total energy (solid) deposited by the circuit model into the 2-D mesh is about 600 kJ. Energy deposited in the plasma through the Lorentz force (dotted) is about equal to the radiated energy (short dash). The kinetic energy (dot-dash) follows the Lorentz force energy until material begins to arrive on-axis which loses kinetic energy while plasma at larger radii continues to gain energy. Joule heating (long dash) is comparatively small.

aluminum wires (previous typical wire numbers had been about 40 or fewer), it was found that the peak power increased and the pulsewidth decreased dramatically. This breakthrough provided opportunities for employing z-pinches in applications which were previously unworkable due to the effects of the instabilities. Simulations with reduced perturbation levels reproduced many of the features of these Al implosions (4,5) and were then done for 120 wire tungsten implosions. A comparison of one such experiment and simulation is shown in Fig. 3. Except for a late time second peak in the radiation, the agreement is good both in current to the peak (the experimental diagnostic fails at or shortly after peak) and in the radiation pulse shape, width, maximum power and total energy. The energy flow in this simulation is illustrated in Fig. 4. It can be seen that resistive (Joule) heating plays only a small role in contributing energy available to be radiated and that the total radiated energy is nearly equal to that provided by the Lorentz force of the current on the plasma, resulting in either acceleration or pdV work. The energy so deposited is about 1.4 greater than that deposited as

kinetic energy in a 0-D (slug) calculation when stopped at a reasonable compression ratio of 20:1 (2-D, more than 400 kJ; 0-D, 185 kJ). The explanation for this discrepancy lies in the radially extended nature of the 2-D plasma rather than in a greater compression ratio (a 0-D compression ratio of more than 1000:1 would be required to produce a kinetic energy equal to that radiated). In essence, the front edge of the extended plasma (which reaches the axis early) loses kinetic energy to internal and then radiation energy, while the rest of the plasma and especially the back edge continues to absorb magnetic field energy through accelerated velocity and pdV work. Similar results apply to the calculation shown in Fig. 1 and have been analyzed in more detail for Pegasus simulations in Ref. 3.

PBFA-Z SIMULATIONS

Predictions for PBFA-Z based upon the latest Saturn results were close to the actual performance seen in the device in early shots, except that current delivery was somewhat lower than expected and the observed radiation pulses had reduced pulse widths. The resultant radiation pulses were matched by a 2-D simulation perturbation level about a factor of five lower than for Saturn simulations (Saturn experiments were matched typically at 15%, the latest PBFA-Z experiments at about 3%). The result for PBFA-Z experiment #26 is shown in Figs. 5 and 6 (Fig. 6 compares pulse shape by scaling and time-shifting the experimental pulse within experimental uncertainty). This experiment used 240, 7.5 μm tungsten wires in a cylindrical array 2-cm long and 4-cm diameter (4.1 mg). The implosion was

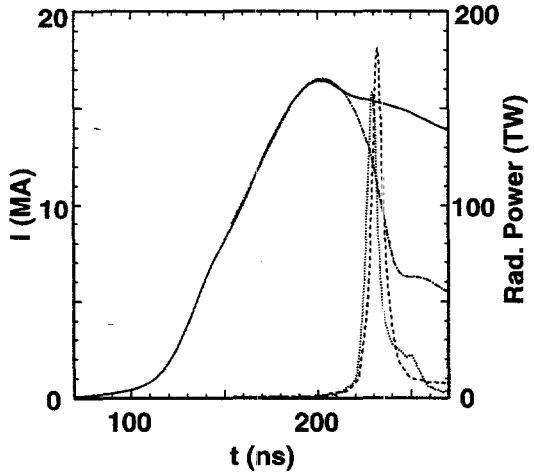

Figure 5. Comparison of experimental (solid, dotted) and simulation (dot-dash, dashed) currents and radiation powers for a 240 wire tungsten PBFA-Z implosion (#26). Experimental current after the peak is unreliable.

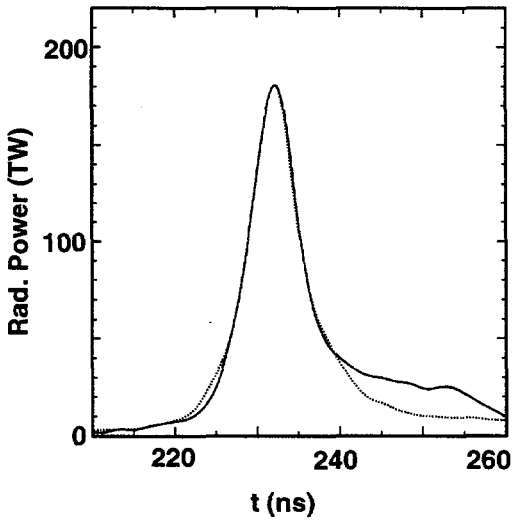

Figure 6. Comparison of experimental (solid) PBFA-Z #26 radiation pulse (scaled to peak 180 TW, shifted +2.7 ns) and 2-D simulation radiation power (dotted).

driven by a peak current of 16.5 MA with an implosion time of about 120 ns resulting in a 7 ns FWHM radiation pulse. The simulation instability growth is illustrated in Fig. 7, which shows the development of a short wavelength phase

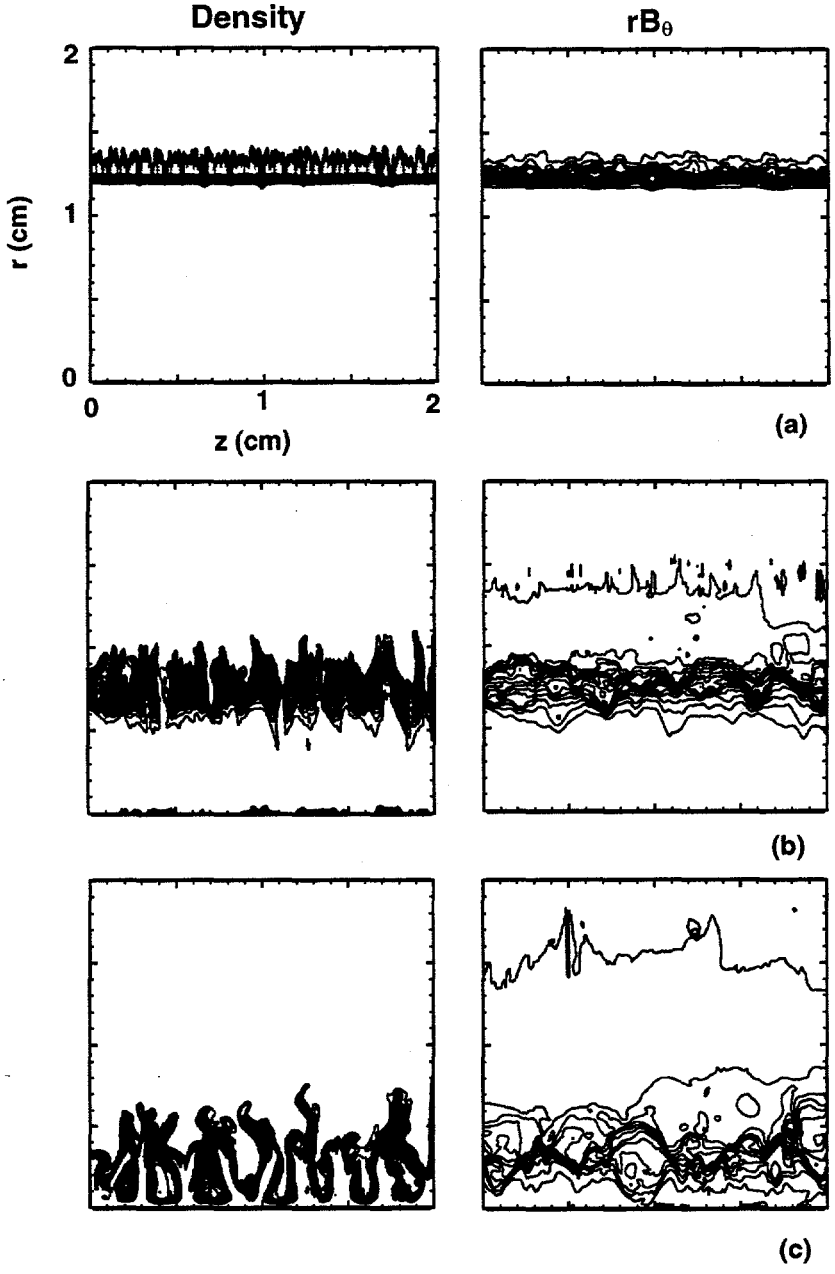

Figure 7. Contours of density and rB_θ for three times in a simulation of the PBFA-Z #26 experiment. The three times shown depict: (a) short wavelength instability development; (b) bubble breakthrough and transition to long wavelength development; (c) maximum instability growth as measured by the fractional involved mass measure.

which saturated without causing the shell to disrupt completely (in contrast to the process described earlier regarding Fig. 1). The initial breakup of the imploding shell is of such short wavelength that the magnetic field does not follow the bubble material being pushed to the axis and instead continues to flow through the spike regions remaining in the shell and the low density regions (remaining from bubble development) between the spike regions. The instability development at this wavelength is now effectively saturated and only a small amount of field and bubble material penetrates inside the plasma shell. Finally, a longer wavelength, comparable in size to the thickened shell, develops the instability growth further. Similar development has been seen in some simulations of Saturn implosions. The fractional involved mass instability measure for this simulation is illustrated in Fig. 8.

Z-PINCH APPLICATIONS

Aside from direct illumination by radiation from the pinch, the electrical return conductor may be used to contain the radiation as a hohlraum, and this may be used to drive experiments. Using both Saturn and PBFA-Z, experiments have been fielded with identical loads in two configurations: "open" (the return conductor had many large slots or return conductor posts were used) and "closed"

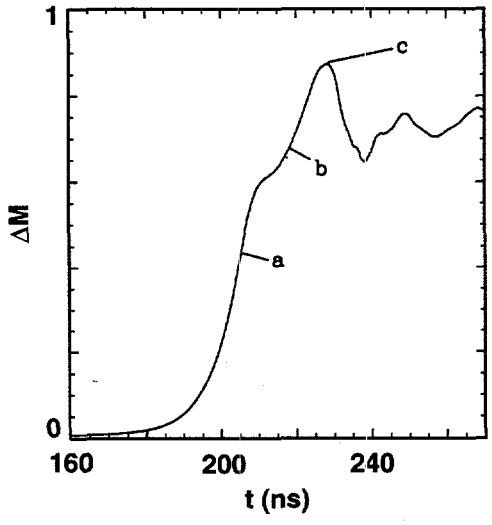

Figure 8. Fractional involved mass as a function of time for the PBFA-Z #26 experiment simulation. The points marked a, b and c correspond to the times of Fig. 7a, 7b and 7c and show short wavelength, long wavelength and the maximum in instability development.

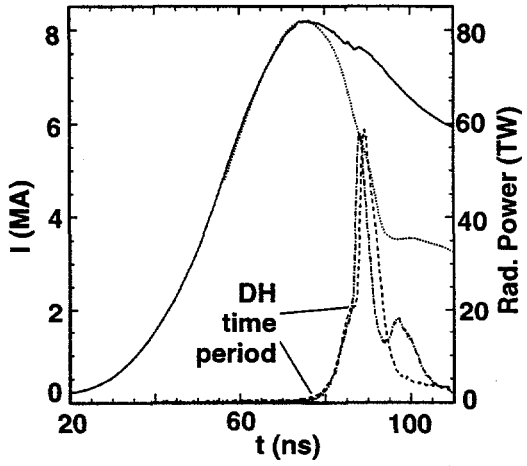

Figure 9. Comparison of experimental (solid, dotted) and simulation (dot-dash, dashed) currents and radiation powers for a Saturn dynamic hohlraum (DH) experiment. The time period when the dynamic hohlraum exists (the "foot" of the radiation pulse) is marked. The tungsten implosion portion of the calculation is the same as that for Fig. 3.

(or "hohlraum," the return conductor was a much as possible an encasing can). The 2-D simulations which included the hohlraum walls (based upon simulations which matched the open configuration experiments) reproduced to a reasonable degree the measured hohlraum temperature. In the latest example, a PBFA-Z 30-mm diameter tungsten implosion in the open configuration was matched by a 2-D simulation (experimental peak power 170 TW, simulation 185 TW). The corresponding closed configuration experiment registered a peak hohlraum temperature of 100 eV and the simulation including the hohlraum walls gave a peak of 94 eV.

Another application of interest is to use the imploding plasma as a radiation case for a hohlraum consisting of a cylindrical (possibly coated) foam on-axis. As the pinch plasma strikes the foam, kinetic energy is converted to thermal energy and radiation fills the foam hohlraum which may then be used for applications experiments. This concept is known as the "dynamic hohlraum" (DH) or "flying radiation case" (FRC)(5,6). The hohlraum will exist for a period of time as the pinch continues to compress the foam. The compression also results in additional heating (pdV work) of the DH. The instabilities play a major role since they can cause bubble material to penetrate the foam early and destroy the integrity of the hohlraum, or cause inhomogeneities in the hohlraum temperature, or cause the radiation case to be leaky because of thinning of the shell in bubble regions. Preliminary experiments of this type were performed on Saturn based upon the tungsten experiments which had produced high radiation powers (85 TW, such at that shown in Fig. 3). Using the simulation which had matched the Saturn tungsten implosions, an aerogel foam was added on-axis in the simulation and the result in shown in Fig. 9. The current again matched the measured current so far as it was reliable, and the radial radiation pulse matched closely in the "foot" region when the dynamic hohlraum exists and also matched the general shape and timing of the pulse as well as the peak power (which occurs after the hohlraum foam has been crushed).

SUMMARY

In conclusion, the methodology of utilizing a 2-D Eulerian RMHD code to simulate an imploding pinch developed for Los Alamos experiments has been successfully applied to Saturn and PBFA-Z implosions using different load materials, masses, radii, implosion times and drive currents. We have obtained results which appear to be in good agreement with measured data, and which explain important features (such as the overall radiated energy). In addition, using the 2-D simulations which have been benchmarked to experiments and then applying them to new circumstances (such as dynamic hohlraum configuration or new drivers such as PBFA-Z) resulted in good agreement with the new experiments, partially fulfilling our desire for design and predictive capability.

There remain limitations in using the 2-D simulations. The code cannot account for 3-D effects when they may become important. As of the present it uses for the radiation treatment a 3-T, gray diffusion model (1). Although such a treatment is not inappropriate for circumstances where the primary effects will come about through MHD dynamics, it is limited in the information which it can self-consistently provide concerning the radiation environment. This limitation is mitigated somewhat in that code "snapshots" in time of density, temperature, etc, can be processed with more sophisticated radiation transport methods (2) to verify consistency in radiation flow with the 3-T model and provide more detailed spectral information. In such a case, we assume that the code has brought us to an appropriate physical configuration and then ask for detailed radiation information which would result from such a configuration. Another limitation is that initial conditions are not known *a priori*, but must instead be determined by finding a perturbation level which will generate the observed data. Although this is not desirable, especially in light of our goal of predictive capability, the circumstance is still one in which physically reasonable conditions early in the simulation develop throughout the implosion in a physically consistent way to produce complex dynamics which generate results that match those of the data.

Despite the limitations, we believe that the 2-D simulations described here have and continue to play an important role in understanding, designing and predicting experimental results in this important field. As our understanding of the complex nature of z-pinches and our ability to simulate the pinches improves, we may expect to make further advances in z-pinch performance and applications by means of such simulations.

REFERENCES

1. Peterson, *et al.*, *Phys. Plasmas* **3**, 368-381 (1996).
2. Matuska, *et al.*, *Phys. Plasmas* **3**, 1415-1429 (1996).
3. Peterson, *et al.*, "Comparison and Analysis of 2-D Simulation Results with Two Implosion Radiation Experiments on the Los Alamos Pegasus I and Pegasus II Capacitor Banks," in *Digest of Technical Papers, Tenth IEEE International Pulsed Power Conference*, 1995, pp. 118-123.
4. Sanford, *et al.*, *Phys. Rev. Lett.* **77**, 5063-5066 (1996).
5. Matzen, M. K., *Phys. Plasmas* **4**, 1519-1527 (1997).
6. Brownell, J. H. and Bowers, R. L., "The Flying Radiation Case," Los Alamos National Laboratory Report LA-UR-97-558, 1997.